





Cite this: *Med. Chem. Commun.*,  
2019, 10, 1457

## Kaolin alleviates the toxicity of graphene oxide for mammalian cells†

Elvira Rozhina, \* Svetlana Batasheva, Anna Danilushkina, Marina Kryuchkova, Marina Gomzikova, Yuliya Cherednichenko, Läysän Nigamatzyanova, Farida Akhatova and Rawil Fakhrullin \*

The development of novel nanoscale vehicles for drug delivery promotes the growth of interest in investigations of interaction between nanomaterials. In this paper, we report the *in vitro* studies of eukaryotic cell physiological response to incubation with graphene oxide and planar kaolin nanoclay. Graphene family materials, including graphene oxide (GO), hold promise for numerous applications due to their unique electronic properties. However, graphene oxide reveals toxicity to some cell lines through an unidentified mechanism. Thus, methods and agents reducing the toxicity of graphene oxide can widen its practical application. We used a colorimetric test, flow cytometry and cell index assay methods to evaluate the effects of separate and combined application of graphene oxide and kaolin on mammalian cells. We have shown that the joint application of graphene oxide and kaolin reduced the negative effects of graphene by almost 20%, most likely because of coagulation of the nanoparticles with each other, which was detected by atomic force microscopy.

Received 29th December 2018,  
Accepted 4th June 2019

DOI: 10.1039/c8md00633d

rsc.li/medchemcomm

### 1. Introduction

Graphene family materials, including graphene oxide (GO), are actively studied and used in electronics,<sup>1,2</sup> composites,<sup>3–6</sup> and catalysis.<sup>7</sup> Incorporation of carbon nanomaterials such as graphene oxide into biomaterial composites of different chemical natures has recently demonstrated to provide very important properties for biomedical applications such as: antibacterial capacity against multidrug-resistant pathogens<sup>8,9</sup> (which was measured by two complementary antimicrobial methods<sup>10</sup>), enhancement of water diffusion and compression performance even with the incorporation of a minuscule amount of carbon nanomaterials,<sup>11,12</sup> and enhancement of a wide range of physical properties of biomaterials of different chemical natures with the incorporation of graphene oxide.<sup>13–16</sup> The urgency of studying the toxicity of graphene oxide is associated with an increasing number of publications on its use as a drug delivery system.<sup>17–19</sup> However, there is already some evidence of the toxicity of graphene oxide for living objects, such as mammalian cells<sup>20–24</sup> and microorganisms.<sup>24</sup> In this regard, the search for methods and agents that reduce the toxicity of graphene oxide is needed.<sup>25</sup> At the same

time, approaches that do not require the physical removal of excess graphene oxide from the medium are relevant. At the moment, there are no reports in the literature on such approaches.

Practical application of kaolin in the production of ceramics<sup>26</sup> and also as a sorbent has been described.<sup>27</sup> It is known that on the edges of kaolin particles, there are both silicon oxide and aluminum oxide, which have a positive charge at low pH values.<sup>28</sup> It is assumed that the use of nanoclay will increase in the future due to its ability to improve the functional properties of many materials.<sup>29,30</sup> The properties of nanomaterials are often tested *in vitro* on cell lines.<sup>31</sup> For example, the effects of GO on the morphology, viability, mortality and membrane integrity were evaluated in human lung epithelial (A549) cells,<sup>32</sup> mouse epithelial cells (JB6Cl41-5a),<sup>33</sup> and colorectal cancer (Colo205, HT-29, HTC-116, and SW480), liver cancer (HepG2), human breast cancer (MCF-7), adenocarcinoma (LNCaP) and human cervical (HeLa B) cell lines.<sup>34</sup> Recently, graphene oxide was found to increase the proliferation of stem cells from human exfoliated deciduous teeth, although it slightly inhibited the cell osteogenic differentiation.<sup>35</sup> The studies on the toxicity of kaolin on cells are few, which also indicates the need to expand such studies. However, very often kaolin is used to collect various agents, for example, to remove heavy metals from the environment,<sup>36</sup> due to its unique physicochemical properties.

In this article, we used planar natural nanoclay kaolin to capture excess graphene oxide in the medium and reduce its

Institute of Fundamental Medicine and Biology, Kazan Federal University, Kremli urami 18, Kazan, Republic of Tatarstan, 420008, Russian Federation.

E-mail: rozhinaelvira@gmail.com, kazanbio@gmail.com

† Electronic supplementary information (ESI) available. See DOI: 10.1039/c8md00633d

toxicity. Using flow cytometry and colorimetric tests, we have shown that the toxic effect of graphene oxide for eukaryotic cells decreased after incubation with kaolin for 24 hours. The interaction of both types of nanoparticles with eukaryotic cells was visualized using enhanced dark-field microscopy. The use of a biocompatible nanoclay can find applications in biomedicine to reduce the intrinsic toxicity of graphene oxide.

## 2. Materials and methods

### 2.1 Materials

Kaolin nanoclay and graphene oxide aqueous solutions, L-glutamine, penicillin, streptomycin and phosphate physiological solution were purchased from Sigma-Aldrich. Annexin V FITC and PI were obtained from Invitrogen (Waltham, Massachusetts, USA).

### 2.2 Particle characterization

The size and zeta potential of nanomaterials were measured using a Zetasizer Nano ZS analyzer (Malvern, UK). Dynamic light scattering is used to measure the size of particles and molecules, while the determination of the zeta potential is based on measuring the electrophoretic mobility of particles using the Doppler effect.

### 2.3 Cell culture

Rat dermal fibroblasts (RDFs) were isolated from the normal skin of a 3 day-old rat. The skin was rinsed with PBS (buffering phosphate physiological solution) three times and cut into pieces (1.5 mm<sup>3</sup>). The skin pieces were put in culture dishes and  $\alpha$ -MEM medium supplemented with 10% (v/v) heat-inactivated fetal bovine serum (FBS), 100 I.U. ml<sup>-1</sup> penicillin and 100 ng ml<sup>-1</sup> streptomycin and L-glutamine was added. Then the culture dish was placed in a humidified incubator containing 5% CO<sub>2</sub> at 37 °C. The cells were harvested with trypsin-EDTA (0.05%, Sigma) when they achieved 80% confluence and seeded into 25 cm<sup>2</sup> culture flasks (Corning). The cells were used in the experiment at passages three-eight. All experiments were carried out in compliance with the procedure protocols approved by Kazan Federal University local ethics committee (protocol #5, date 27.05.2014) according to the rules adopted by Kazan Federal University and Russian Federation Laws. The human colon cancer cells (HCT116) were obtained from the American Type Culture Collection (ATCC, USA). Before the experiments, the cells were seeded in 6-well plates with a number of 100 thousand cells per well. After 24 hours of incubation, nanomaterials were added into each well to a required concentration of 50–200  $\mu$ g ml<sup>-1</sup>. In the variant where a mixture (1 : 1) of graphene oxide and kaolin was added to the cells, nanomaterials were mixed 12 h prior to cell treatment. After 24 hours of combined incubation, the toxic effect of nanoparticles was analyzed.

### 2.4 Flow cytometry analysis

Analysis of kaolin and graphene oxide toxicity and apoptosis-inducing potential on the cells was carried out with the flow cytometry method using a BD FACS (USA) instrument according to a standard protocol provided by the staining kit manufacturer. The cells were stained with a Dead Cell Apoptosis kit with Annexin V FITC and PI (propidium iodide) for flow cytometry (Invitrogen). During the analysis, the number of annexin positive cells (green) and propidium iodide positive cells (red) was determined.

### 2.5 MTT test

The HCT116 cells (2000 per well) were placed in a 96-well plate with  $\alpha$ -MEM medium. After 24 hours, 20  $\mu$ l of MTT (3-(4,5-dimethylthiazol-2-yl)-2,5-diphenyltetrazolium bromide, Sigma) solution was added and incubated for 4 hours. The supernatant was removed and 200  $\mu$ l of DMSO (dimethyl sulfide, Sigma) was added into each well. Finally, absorbance was recorded at 540 nm using a MultiScan reader (Thermo Scientific, USA).

### 2.6 Cell index assay

Cell growth was measured with an xCELLigence real-time cell analyzer (Roche, Germany). The cells were grown for 4 days in special culture plates (E-plate) and each day, the cell impedance was measured between the sensor electrodes every 60 min, allowing us to estimate the cell density. The background value was measured in an E-plate, containing 100  $\mu$ l of culture medium. HCT-116 cells were seeded as 5000 cells per well and in 24 h, kaolin (100  $\mu$ g ml<sup>-1</sup>), graphene oxide (100  $\mu$ g ml<sup>-1</sup>) and a mixture of kaolin with graphene oxide (100 and 200  $\mu$ g ml<sup>-1</sup>) were added. All concentrations are final concentrations of nanomaterials in culture medium.

### 2.7 Imaging

AFM images were obtained using a Dimension Icon (Bruker, USA) microscope, operating in the PeakForce Tapping mode. ScanAsyst-air probes (Bruker) were used (115  $\mu$ m, tip radius 2 nm, spring constant (0.4 N m<sup>-1</sup>)). The images were obtained at 512–1024 lines per scan at 0.8–0.9 Hz scan rate in order to provide high resolution of images and mapping of mechanical properties. Images were collected as peak force error and adhesion images. The data obtained were processed using Nanoscope Analysis v.1.7. software (Bruker). Dark field microscopy images were obtained using a Cytoviva® high annular aperture dark-field condenser attached to an Olympus BX51 upright microscope. The cells were trypsinized, washed with buffer (PBS) and put on a coverslip without fixation. The exposure time was 100  $\mu$ s. Images were analyzed using Exponent 7 imaging software (Dage-MTI).

### 2.8 Statistical analysis

Results of three independent experiments each including 3 or more replicas are presented in figures and tables as means

± SD. Statistical analysis was performed using the Student's *t*-test and differences were considered significant at  $p < 0.05$ .

### 3. Results and discussion

At the first stage, the hydrodynamic diameters and zeta-potentials of nanoparticles were characterized using laser light scattering. The results of measurements are shown in Table 1. We found that sizes of the individual nanoparticles corresponded well to those reported earlier.<sup>37</sup>

Nanoparticles formed well-dispersed aggregates, which could be visualized using dark-field (DF) microscopy (Fig. 1). Imaging of nanoparticles using dark-field microscopy is an informative approach for examination of the nanoparticle distribution on cellular membranes and inside the cells,<sup>38</sup> facilitating the detection of nanoparticles *in situ*, without any pre-treatment or fixation of cells. We found that both types of nanomaterials and their mixture were stable in water at room temperature.

A previous report suggests that positively-charged sites may exist on the edges of kaolin plates, because the charges of amphoteric octahedral Al-OH sites at the broken edges and exposed hydroxyl-terminated planes of kaolin depend on pH.<sup>39</sup> At pH below 6–6.5, a significant fraction of the edge sites of kaolin must be positively charged in spite of the overall negative charge of the clay plate.<sup>39</sup> In our work, the pH values of the kaolin and graphene oxide suspensions were within the acidic pH range (pH = 5), therefore, the terminal regions of the planar nanoclay were most likely positively charged, favouring sorption of negatively charged graphene oxide particles when graphene oxide was mixed with kaolin. Usually, the detoxifying ability of clay minerals such as montmorillonite and kaolin is associated with their cation exchange capacity, allowing protection of living organisms from the negative effect of heavy metals, for example, cadmium (Cd).<sup>36</sup> However, kaolin exhibits one of the lowest cation exchange capacities as compared to other types of nanoclays (montmorillonite, halloysite, *etc.*).<sup>40</sup> Alternatively, in this work, we tried to take advantage of high sorption properties of kaolin<sup>41</sup> to apply it for improvement of graphene oxide toxicity towards mammalian cells. As the first step, we estimated the absorption of the nanomaterials by the cells.

Using enhanced dark-field microscopy, we visualised the internalization of both types of nanomaterials by human colon cancer cells (HCT116). HCT116 cells were incubated with nanomaterials for 24 h, then they were detached with trypsin, and cell suspension in buffer was visualised. The nanoparticles and their mixture were suspended in phosphate

buffer and added to the medium at a concentration of 100  $\mu\text{g ml}^{-1}$ . We found that in all variants, the nanoparticles were visualised inside the cells (Fig. 2).

The time-resolved interactions of nanoparticles with non-fixed viable cells were also imaged using dark-field microscopy in real-time video recording mode (ESI† 1–3), and the typical shots from the videos are presented in Fig. 3. There have been previous reports of graphene oxide uptake by human fibroblasts,<sup>42</sup> and graphene oxide modified with polyethylene-glycol (PEG) entered mesenchymal stem cells and was distributed in the cytosol.<sup>43</sup> Kaolin was also found to be strongly adhered to the cell surface and efficiently taken up by different cell types.<sup>44</sup> The visualisation of graphene oxide and kaolin nanoparticles alone and in mixture using dark-field microscopy demonstrates that they are actively internalized by cells, and it is likely that the binding of these nanoparticles occurs both on the membranes and in the cytosol.

The influence of nanomaterials on the proliferative activity of HCT116 cells was determined by two different methods. The MTT test was used to evaluate the activity of cellular hydrogenases<sup>45</sup> 24 hours after nanomaterial addition and cell impedance was measured during cell growth with nanomaterials for 96 h. We have shown that the incubation of HCT-116 cells with graphene oxide reduced the number of living cells by almost 40% in comparison with the control (Fig. 4A). Reduction of the metabolic activity of HCT116 cells by 100  $\mu\text{g ml}^{-1}$  graphene oxide is in good agreement with a loss of cell viability of A549 cells induced by similar graphene oxide concentrations<sup>32</sup> and the results of Wang *et al.* (2011)<sup>42</sup> who found that the dose of graphene oxide of more than 50  $\mu\text{g mL}^{-1}$  exhibits obvious cytotoxicity to human fibroblast cells. At the same time, the toxicity of graphene oxide nanosheets is dependent not only on the dose but also on the size of the particles.<sup>32</sup>

Joint application of graphene and kaolin reduced the negative effect of graphene by almost 20% (Fig. 4A). However, although 100  $\mu\text{g ml}^{-1}$  of the added 1:1 mixture of kaolin and graphene oxide suspension apparently contained the same number of particles as separate 100  $\mu\text{g ml}^{-1}$  kaolin or graphene suspensions, the concentration of each nanoparticle species in the mixture was only 50  $\mu\text{g ml}^{-1}$ . Thus, the question arose as to whether the reduced toxicity of graphene oxide after its mixing with kaolin was related to detoxifying effect of kaolin or to lower graphene oxide concentration. Then, we increased the concentration of the added 1:1 kaolin-graphene oxide mixture to 200  $\mu\text{g ml}^{-1}$ , so graphene oxide and kaolin contents in the mixture were the same as in separate kaolin and graphene oxide suspensions. Additionally, we increased the incubation time of cells with nanomaterials up to 72 h to track the long-term changes in cell proliferative activity (Fig. 4B). We have found that kaolin reduces the toxic effect of equal concentrations of graphene oxide after 72 hours of joint incubation. The decrease in graphene toxicity even when high levels of kaolin and graphene are used coincides with the results obtained earlier.<sup>37</sup>

**Table 1** The average hydrodynamic diameter and zeta potential of nanomaterials dispersed in deionized water

No.	Sample	Size, nm ± SD	Zeta-potential, mV ± SD
1	Graphene oxide (GO)	1629.0 ± 201.6	-38.8 ± 3.4
2	Kaolin (KNPs)	2203.0 ± 22.3	-22.0 ± 0.7
3	GO + KNPs	1097.0 ± 81.9	-45.6 ± 0.8

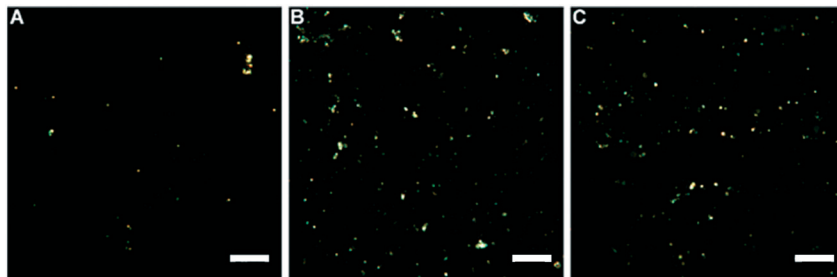


Fig. 1 Dark-field microscopy images of nanoparticles: (A) kaolin (KNPs); (B) graphene oxide (GO); (C) graphene oxide incubated with kaolin. Scale bar: 20  $\mu\text{m}$ .

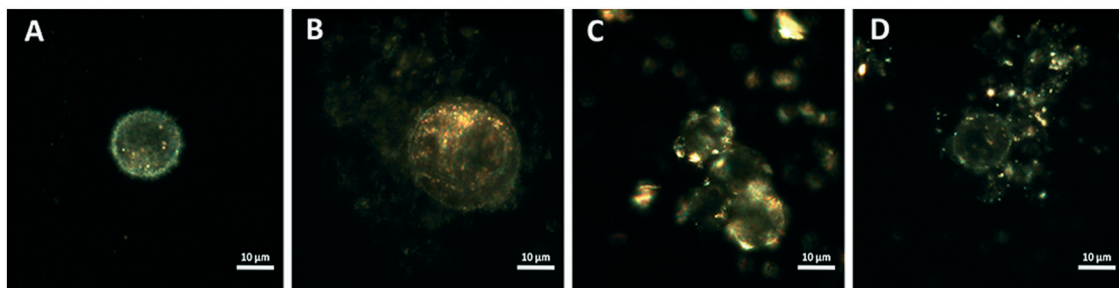


Fig. 2 Dark-field microscopy images of HCT116 cells: non-treated (A), treated with graphene oxide ( $100 \mu\text{g mL}^{-1}$ ) (B), treated with kaolin ( $100 \mu\text{g mL}^{-1}$ ) (C), and treated with a mixture of kaolin and graphene oxide ( $100 \mu\text{g mL}^{-1}$ ) (D).

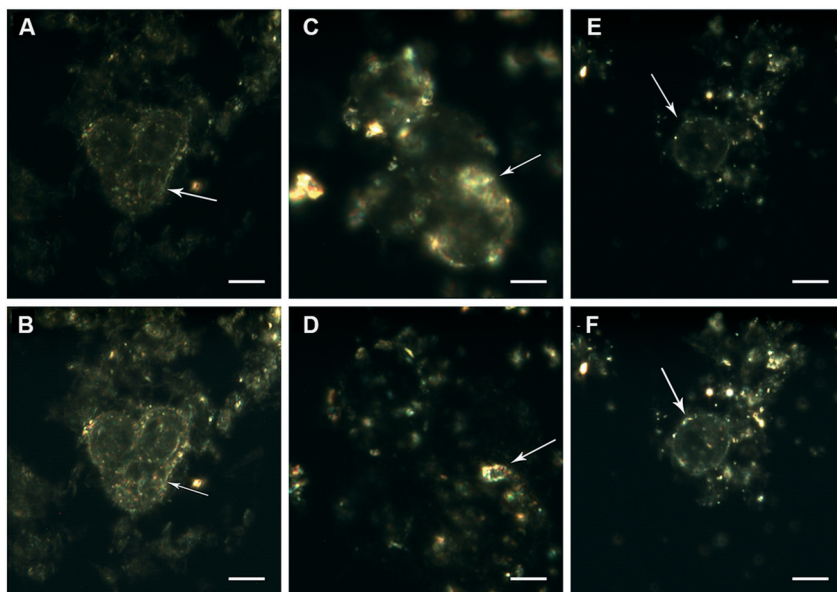


Fig. 3 Visualisation of the interaction of nanoparticles with HCT116 cells using dark-field microscopy in the time series mode: treated with graphene oxide ( $100 \mu\text{g mL}^{-1}$ ) (A and B), treated with kaolin ( $100 \mu\text{g mL}^{-1}$ ) (C and D), and treated with a mixture of kaolin and graphene oxide ( $100 \mu\text{g mL}^{-1}$ ) (E and F). Scale bar: 10  $\mu\text{m}$ . Time of exposure to nanoparticles before video recording was 1 hour. Arrows indicate the nanoparticles adhered to the cell surface.

There are conflicting data on the effect of graphene oxide on the viability of living organisms.<sup>34,46–48</sup> We believe that different biological entities vary in their susceptibility to graphene oxide, so we decided to assess the effect of graphene oxide, kaolin and their combined effect on the induction of apoptosis in primary cells. To evaluate the effect

of the investigated nanoparticles on rat dermal fibroblast (RDF) cells, a Dead Cell Apoptosis kit containing Annexin V FITC and PI (Invitrogen) was used (Fig. 4C–F). It is known that annexin has a high affinity for extracellular phosphatidylserine (PS), which appears on the outer surface of the plasma membrane at the early stage of apoptosis. The

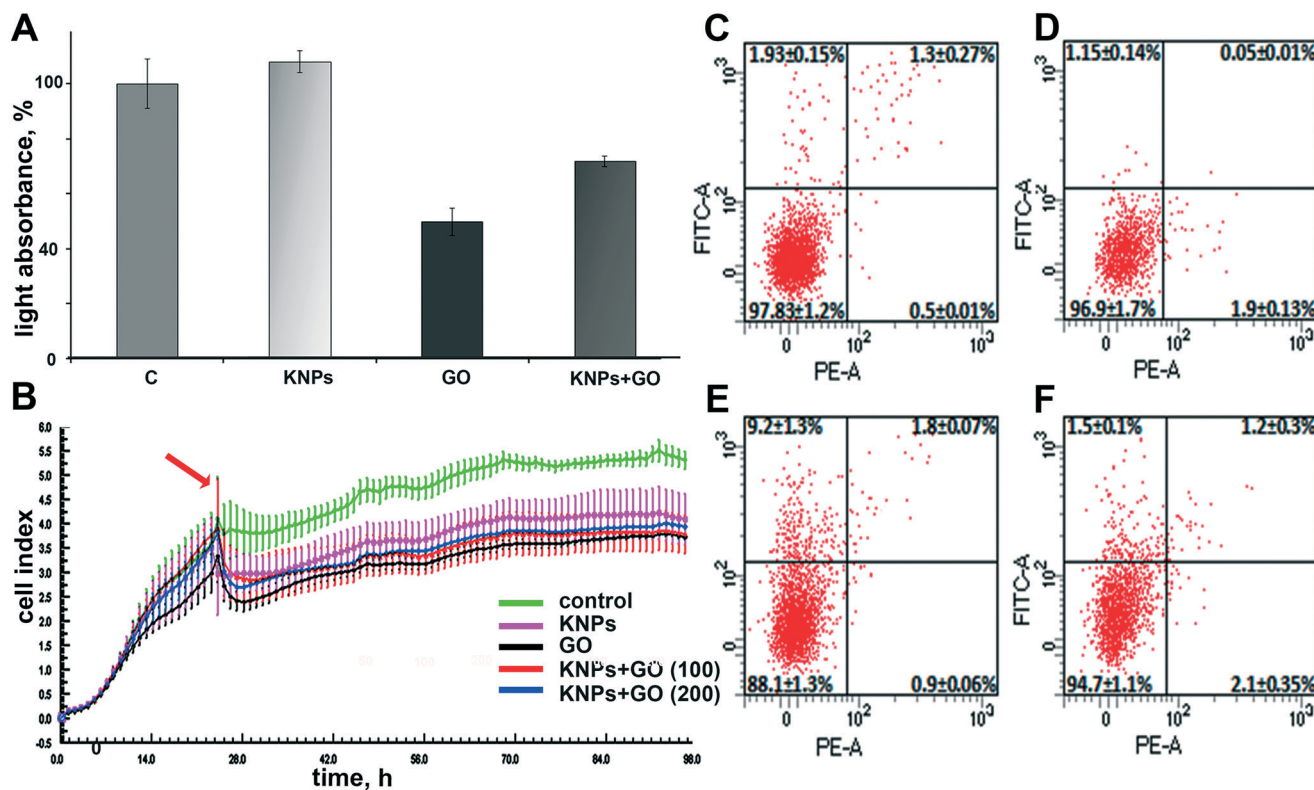


Fig. 4 Quantitative analysis of enzymatic activity in HCT-116 cells (MTT-test) with nanoparticles in  $100 \mu\text{g ml}^{-1}$  concentration (A); HCT-116 cell growth assessed by measurement of cell impedance; the arrow indicates the moment in which nanomaterials were added (B); flow cytometry data demonstrating the viability of RDF cells: intact RDF (C), RDF treated with kaolin ( $100 \mu\text{g ml}^{-1}$ ) (D), RDF treated with GO ( $100 \mu\text{g ml}^{-1}$ ) (E), and RDF treated with GO-KNPs ( $100 \mu\text{g ml}^{-1}$ ) (F). The data demonstrated that addition of kaolin + graphene oxide mixture to the cells reduces the toxicity of graphene.

use of annexin, associated with the fluorophore, allows visualization of cells undergoing apoptotic death.

The results of the analysis showed that in the experiments with the introduction of graphene oxide, the proportion of apoptotic cells exceeded 9%, which suggested the low toxicity of graphene oxide for RDFs in the concentration under study and the realization of the toxic effect of graphene oxide through apoptosis. The lower percentage of dead cells observed in RDF cells compared to that of the HCT-116 cell line might be related to different sensitivities of various cell types to nanomaterials, repeatedly observed in nanotoxicological studies.<sup>34,44</sup>

The negative effects of graphene can be associated with both the membrane exposure and internalization of nanoparticles, indicating that graphene oxide can induce reactive oxygen species (ROS) generation in the culture media, which promotes ROS production inside the cells.<sup>32</sup> Kaolin did not exert any toxic effects on cells and the measured proportion of apoptotic cells is comparable with that in the control. Notably, the combined application of kaolin and graphene oxide reduced the toxic effect of the latter, and the percentage of cells in apoptosis significantly decreased. The determination of the mechanism by which kaolin reduces the toxic effect of graphene oxide to cells requires additional studies. One of the probable mechanisms of alleviated graphene oxide toxic-

ity in the presence of kaolin could be the sorption of graphene oxide nanosheets by kaolin plates as was proposed earlier.<sup>37</sup> Such sorption can decrease graphene oxide uptake by cells or prevent graphene oxide induced ROS formation in the media or inside the cells.

The morphology of particles is an important factor in determining the toxicity of nanomaterials.<sup>49</sup> Atomic force microscopy characterization of the morphologies and sizes of the nanomaterials studied demonstrated that both types of nanoparticles were of planar shape (Fig. 5).

Using the atomic force microscopy, we have shown the coagulation of graphene oxide nanoparticles with kaolin. The assumption that graphene oxide plates are attached to the surface of kaolin was confirmed by the adhesion data. The adhesion of pure kaolin is much larger (about 6.5–9.7 nN) than the adhesion of pure graphene oxide (about 4.2–4.5 nN). The adhesion value of the kaolin after its mixing with graphene oxide (3.7–4.2 nN) becomes closer to the adhesion value of graphene, suggesting the adsorption of graphene oxide by kaolin. This is also confirmed by the change in the hydrodynamic dimensions of particles (Table 1) and dark-field microscopy imaging. Our results are in contrast to those of Zhao *et al.* (2015),<sup>50</sup> who found no adsorption of graphene oxide sheets by montmorillonite and kaolinite and related this effect to the impossible electrostatic interaction between the particles

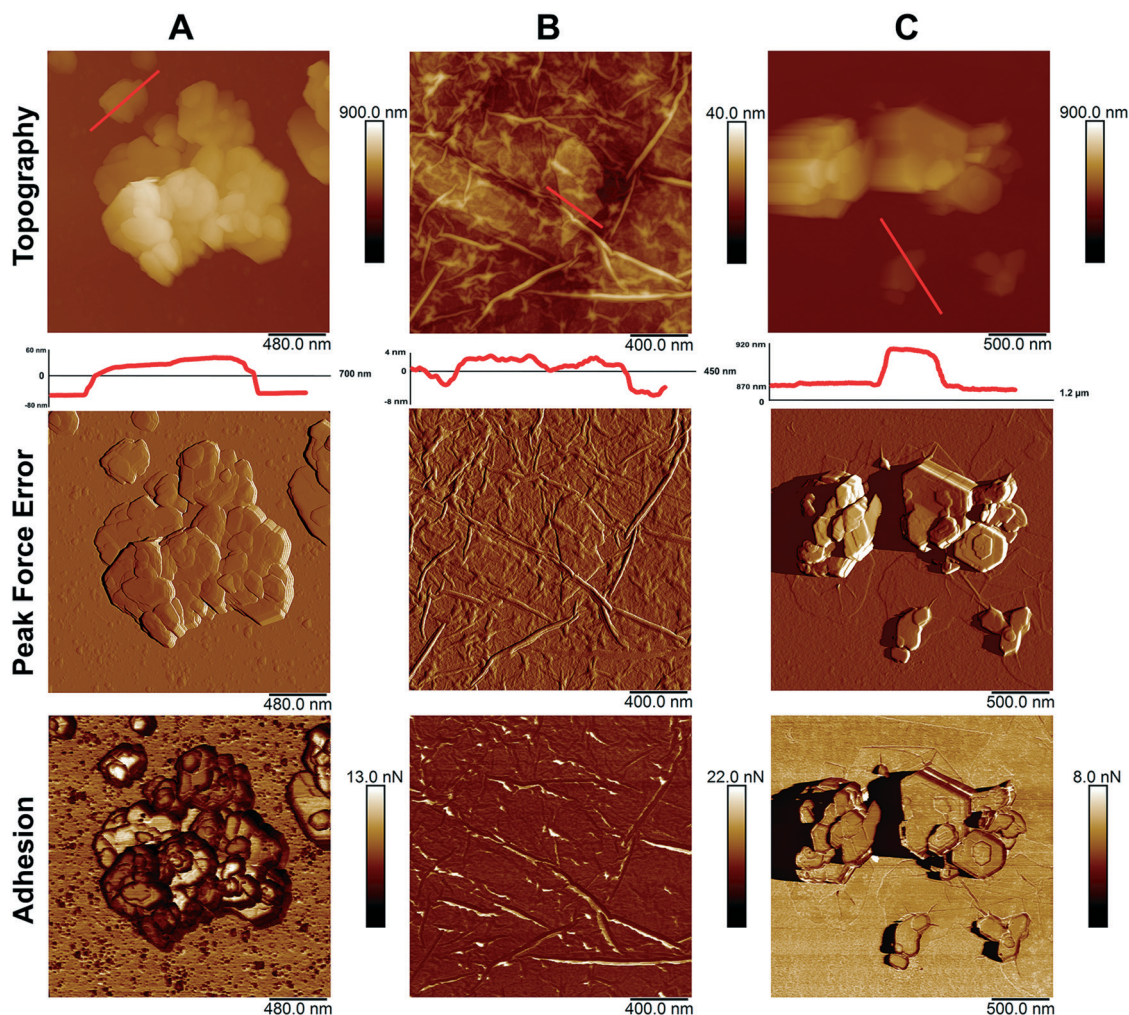


Fig. 5 Atomic force microscopy images of: kaolin (A); graphene oxide (B); kaolin with graphene oxide (C).

because of the negative zeta potentials of both interacting partners. However, using atomic force microscopy and sedimentation analysis, earlier it was clearly demonstrated that planar kaolin nanoparticles strongly aggregated with graphene oxide plates in an aqueous medium.<sup>37</sup> Kaolin coagulated with graphene oxide in water, forming relatively large conglomerates, which resulted in the reduced negative effects of graphene oxide to ciliate protozoan *Paramecium caudatum*.<sup>37</sup> Moreover, kaolinite demonstrated better sorption properties towards graphene oxide (compared to montmorillonite or illite) and inhibited the transport of graphene oxide in saturated porous media.<sup>39</sup> The inconsistency between the results of various experiments on kaolin sorption capacity towards graphene oxide can be related to differences in the experimental procedures used, including the pH of the medium where nanomaterials interact, which results in varying numbers of accessible positively charged sites on kaolin edges. As it was described earlier,<sup>39</sup> pH exceeding 6–6.5 is unfavorable for the formation of positive sites on kaolin plate edges. In our work and that by Kryuchkova and Fakhrullin (2018),<sup>37</sup> kaolin and graphene oxide were co-incubated at a

pH level of about 5 before being added to living cells, and formation of positively charged sites on kaolin was highly probable under such conditions, contributing to binding of negatively charged graphene oxide sheets by kaolin plates. It is interesting that bound graphene oxide is obviously retained by kaolin even after the transfer of the aggregated particles to cell containing medium with higher pH (>7), as evidenced by lower toxicity of the graphene oxide–kaolin mixture compared with pure graphene oxide towards *P. caudatum*<sup>37</sup> or mammalian cells.

## 4. Conclusions

We have shown that graphene oxide induces apoptosis in rat dermal fibroblasts and reduces the proliferative activity in human colon carcinoma cells (HCT116). Natural nanoclay did not exert a toxic effect on mammalian cells in the concentration under study. Also, kaolin reduced the toxic effect of graphene on eukaryotic cells and did not prevent its penetration into the cells. Cultivation of HCT-116 cells with graphene oxide reduced the number of living cells by almost

40% relative to the control, but the combined application of graphene oxide and kaolin reduced the negative effect of graphene oxide for the cells by almost 20%. The unique properties of graphene based materials hold promise for versatile practical applications, including that in biomedicine. As the use of graphene oxide as a vehicle for drug delivery is restrained by its toxicity, combining it with kaolin could help to resolve this problem.

## Conflicts of interest

There are no conflicts to declare.

## Acknowledgements

This work is performed according to the Russian Government Program of Competitive Growth of Kazan Federal University. This work was funded by the subsidy (project 16.2822.2017/4.6) allocated to the Kazan Federal University for the state assignment in the sphere of scientific activities and funded by the Russian presidential grant MK-4498.2018.4 and RFBR 18-29-25057 project.

## References

- W. Cai, Y. Zhu, X. Li, R. D. Piner and R. S. Ruoff, Large area few-layer graphene/graphite films as transparent thin conducting electrodes, *Appl. Phys. Lett.*, 2009, **95**(12), 123115.
- X. Li, Y. Zhu, W. Cai, M. Borysiak, B. Han, D. Chen, R. D. Piner, L. Colombo and R. S. Ruoff, Transfer of large-area graphene films for high-performance transparent conductive electrodes, *Nano Lett.*, 2009, **9**(12), 4359–4363.
- S. Stankovich, D. A. Dikin, G. H. Dommett, K. M. Kohlhaas, E. J. Zimney, E. A. Stach, R. D. Piner, S. T. Nguyen and R. S. Ruoff, Graphene-based composite materials, *Nature*, 2006, **442**(7100), 282–286.
- S. Park and R. S. Ruoff, Chemical methods for the production of graphenes, *Nat. Nanotechnol.*, 2009, **4**(4), 217–224.
- M. Fang, K. Wang, H. Lu, Y. Yang and S. Nutt, Covalent polymer functionalization of graphene nanosheets and mechanical properties of composites, *J. Mater. Chem.*, 2009, **19**(38), 7098–7105.
- Y. Chen, Y. Qi, Z. Tai, X. Yan, F. Zhu and Q. Xue, Preparation, mechanical properties and biocompatibility of graphene oxide/ultrahigh molecular weight polyethylene composites, *Eur. Polym. J.*, 2012, **48**(6), 1026–1033.
- C. L. Su and K. P. Loh, Carbocatalysts: graphene oxide and its derivatives, *Acc. Chem. Res.*, 2013, **46**, 2275–2285.
- M. Martí, B. Frígols, B. Salesa and Á. Serrano-Aroca, Calcium alginate/graphene oxide films: Reinforced composites able to prevent *Staphylococcus aureus* and methicillin-resistant *Staphylococcus epidermidis* infections with no cytotoxicity for human keratinocyte HaCaT cells, *Eur. Polym. J.*, 2019, **110**, 14–21.
- B. Salesa, M. Martí, B. Frígols and Á. Serrano-Aroca, Carbon nanofibers in pure form and in calcium alginate composites films: New cost-effective antibacterial biomaterials against the life-threatening multidrug-resistant *Staphylococcus epidermidis*, *Polymer*, 2019, **11**(3), 453.
- M. Martí, B. Frígols and A. Serrano-Aroca, Antimicrobial characterization of advanced materials for bioengineering applications, *J. Visualized Exp.*, 2018, **138**, e57710.
- Á. Serrano-Aroca, J.-F. Ruiz-Pividal and M. Llorens-Gámez, Enhancement of water diffusion and compression performance of crosslinked alginate films with a minuscule amount of graphene oxide, *Sci. Rep.*, 2017, **7**(1), 11684.
- M. Llorens-Gámez and Á. Serrano-Aroca, Low-cost advanced hydrogels of calcium alginate/carbon nanofibers with enhanced water diffusion and compression properties, *Polymer*, 2018, **10**(4), 405.
- Á. Serrano-Aroca, L. Iskandar and S. Deb, Green synthetic routes to alginate-graphene oxide composite hydrogels with enhanced physical properties for bioengineering applications, *Eur. Polym. J.*, 2018, **103**, 198–206.
- F. Sánchez-Correa, C. Vidaurre-Agut, Á. Serrano-Aroca and A. J. Campillo-Fernández, Poly(2-hydroxyethyl acrylate) hydrogels reinforced with graphene oxide: Remarkable improvement of water diffusion and mechanical properties, *J. Appl. Polym. Sci.*, 2018, **135**(15), 46158.
- Á. Serrano-Aroca and S. Deb, Synthesis of irregular graphene oxide tubes using green chemistry and their potential use as reinforcement materials for biomedical applications, *PLoS One*, 2017, **12**(9), e0185235.
- A. L. Rivera-Briso and Á. Serrano-Aroca, Poly(3-Hydroxybutyrate-co-3-Hydroxyvalerate): Enhancement strategies for advanced applications, *Polymer*, 2018, **10**(7), 732.
- Z. Liu, J. T. Robinson, X. Sun and H. Dai, PEGylated nanographene oxide for delivery of water-insoluble cancer drugs, *J. Am. Chem. Soc.*, 2008, **130**(33), 10876–10877.
- X. Sun, Z. Liu, K. Welsher, J. T. Robinson, A. Goodwin, S. Zaric and H. Dai, Nano-graphene oxide for cellular imaging and drug delivery, *Nano Res.*, 2008, **1**(3), 203–212.
- K. Lee, P. Lo, G. Lee, J. Zheng and E. Cho, Carboxylated carbon nanomaterials in cell cycle and apoptotic cell death regulation, *J. Biotechnol.*, 2019, **296**, 14–21.
- A. Sasidharan, S. Swaroop, P. Chandran, S. Nair and M. Koyakutty, Cellular and molecular mechanistic insight into the DNA-damaging potential of few-layer graphene in human primary endothelial cells, *Nanomed.: Nanotechnol., Biol. Med.*, 2016, **12**(5), 1347–1355.
- T. A. Tabish, M. Z. I. Pranjol, H. Hayat, A. A. M. Rahat, T. M. Abdullah, J. L. Whatmore and S. Zhang, In vitro toxic effects of reduced graphene oxide nanosheets on lung cancer cells, *Nanotechnology*, 2017, **28**(50), 504001.
- Y. Li, Y. Liu, Y. Fu, T. Wei, L. Le Guyader, G. Gao, R.-S. Liu, Y.-Z. Chang and C. Chen, The triggering of apoptosis in macrophages by pristine graphene through the MAPK and TGF-beta signaling pathways, *Biomaterials*, 2012, **33**(2), 402–411.
- K.-H. Liao, Y.-S. Lin, C. W. Macosko and C. L. Haynes, Cytotoxicity of Graphene Oxide and Graphene in Human Erythrocytes and Skin Fibroblasts, *ACS Appl. Mater. Interfaces*, 2011, **3**(7), 2607–2615.

- 24 M. Chen, Y. Sun, J. Liang, G. Zeng, Z. Li, L. Tang, Y. Zhu, D. Jiang and B. Song, Understanding the influence of carbon nanomaterials on microbial communities, *Environ. Int.*, 2019, **16**, 690–698.
- 25 M. Chen, X. Qin and G. Zeng, Biodegradation of Carbon Nanotubes, Graphene, and Their Derivatives, *Trends Biotechnol.*, 2017, **35**(9), 836–846.
- 26 P. A. Ciullo, *Industrial Minerals and Their Uses: A Handbook and Formulary*, Noyes Publication, 1996.
- 27 F. Arias and T. K. Sen, Removal of zinc metal ion (Zn<sup>2+</sup>) from its aqueous solution by kaolin clay mineral: A kinetic and equilibrium study, *Colloids Surf., A*, 2009, **348**(1–3), 100–108.
- 28 A. A. Zaman, R. Tsuchiya and B. M. Moudgil, Adsorption of a low molecular weight polyacrylic acid on silica, alumina and kaolin, *J. Colloid Interface Sci.*, 2002, **256**, 73–78.
- 29 B. Chen and J. R. G. Evans, Impact strength of polymer-clay nanocomposites, *Soft Matter*, 2009, **5**, 3572–3584.
- 30 X. Lai, M. Agarwal, Y. Lvov, C. Pachpande, K. Varahramyan and F. Witzmann, Proteomic profiling of halloysite clay nanotube exposure in intestinal cell co-culture, *J. Appl. Toxicol.*, 2013, **33**(11), 1316–1329.
- 31 R. F. Kamaliev, I. R. Ishmukhametov, S. N. Batasheva, E. V. Rozhina and R. F. Fakhrullin, Uptake of halloysite clay nanotubes by human cells: Colourimetric viability tests and microscopy study, *Nano-Struct. Nano-Objects*, 2018, **15**, 54–60.
- 32 Y. Chang, S.-T. Yang, J.-H. Liu, E. Dong, Y. Wang, A. Cao, Y. Liu and H. Wang, In vitro toxicity evaluation of graphene oxide on A 549 cells, *Toxicol. Lett.*, 2011, **200**(3), 201–210.
- 33 Y. Wang, Z. Li, D. Hu, C.-T. Lin, J. Li and Y. Lin, Aptamer/graphene oxide nanocomplex for in situ molecular probing in living cells, *J. Am. Chem. Soc.*, 2010, **132**(27), 9274–9276.
- 34 M. Kutwin, E. Sawosz, S. Jaworski, M. Wierzbicki, B. Strojny, M. Grodzik, M. Sosnowska, M. Trzaskowski and A. Chwalibog, Nanocomplexes of Graphene Oxide and Platinum Nanoparticles against Colorectal Cancer Colo205, HT-29, HTC-116, SW480, Liver Cancer HepG2, Human Breast Cancer MCF-7, and Adenocarcinoma LNCaP and Human Cervical Hela B Cell Lines, *Materials*, 2019, **12**, 909.
- 35 X. Yang, Q. Zhao, Y. Chen, Y. Fu, S. Lu, X. Yu, D. Yu and W. Zhao, Effects of graphene oxide and graphene oxide quantum dots on the osteogenic differentiation of stem cells from human exfoliated deciduous teeth, *Artif. Cells, Nanomed., Biotechnol.*, 2019, **47**(1), 822–832.
- 36 H. Babich and G. Stotzky, Reductions in the toxicity of cadmium to microorganisms by clay minerals, *Appl. Environ. Microbiol.*, 1977, **33**(3), 696–705.
- 37 M. Kryuchkova and R. Fakhrullin, Kaolin Alleviates Graphene Oxide Toxicity, *Environ. Sci. Technol. Lett.*, 2018, **5**(5), 295–300.
- 38 F. Akhatova, A. Danilushkina, G. Kuku, M. Saricam, M. Culha and R. Fakhrullin, Simultaneous intracellular detection of plasmonic and non-plasmonic nanoparticles using dark-field hyperspectral microscopy, *Bull. Chem. Soc. Jpn.*, 2018, **91**(11), 1640–1645.
- 39 T. Lu, T. Xia, Y. Qi, C. Zhang and W. Chen, Effects of clay minerals on transport of graphene oxide in saturated porous media, *Environ. Toxicol. Chem.*, 2017, **36**, 655–660.
- 40 H. H. Murray, *Applied Clay Mineralogy: Occurrences, Processing and Applications of Kaolins, Bentonites, Palygorskites, Sepiolite, and Common Clays*, Elsevier, 1st edn, 2007.
- 41 M. E. Awad, A. Lopez-Galindo, M. Setti, M. M. El-Rahmany and C. V. Iborra, Kaolinite in pharmaceuticals and biomedicine, *Int. J. Pharmacol.*, 2017, **533**(1), 34–48.
- 42 K. Wang, J. Ruan, H. Song, J. Zhang, Y. Wo, S. Guo and D. Cui, Biocompatibility of graphene oxide, *Nanoscale Res. Lett.*, 2011, **6**(1), 8.
- 43 S. Syama, C. P. Aby, T. Maekawa, D. Sakthikumar and P. V. Mohanan, Nano-bio compatibility of PEGylated reduced graphene oxide on mesenchymal stem cells, *2D Mater.*, 2017, **4**(2), 025066.
- 44 Y. Li, A. M. Sawvel, Y.-S. Jun, S. Nownes, M. Ni, D. Kudela, G. D. Stucky and D. Zink, Cytotoxicity and potency of mesocellular foam-26 in comparison to layered clays used as hemostatic agents, *Toxicol. Res.*, 2013, **2**, 136.
- 45 M. V. Berridge, P. M. Herst and A. S. Tan, Tetrazolium dyes as tools in cell biology: New insights into their cellular reduction, *Int. J. Pharmacol.*, 2005, **11**, 127–152.
- 46 M. Kryuchkova, A. Danilushkina, Y. Lvov and R. Fakhrullin, Evaluation of toxicity of nanoclays and graphene oxide: in vivo A Paramecium caudatum study, *Environ. Sci.: Nano*, 2016, **3**(2), 442–452.
- 47 L. Horváth, A. Magrez, M. Burghard, K. Kern, L. Forró and B. Schwaller, Evaluation of the toxicity of graphene derivatives on cells of the lung luminal surface, *Carbon*, 2013, **64**, 45–60.
- 48 A. Karmakar, T. Mallick, S. Das and N. A. Begum, Naturally occurring green multifunctional agents: Exploration of their roles in the world of graphene and related systems, *Nano-Struct. Nano-Objects*, 2018, **13**, 1–20.
- 49 J. Petkovic, B. Zegura, M. Stevanovic, N. Drnovsek, D. Uskokovic, S. Novak and M. Filipic, DNA damage and alterations in expression of DNA damage responsive genes induced by TiO<sub>2</sub> nanoparticles in human hepatoma HepG2 cells, *Nanotoxicology*, 2011, **5**, 341–353.
- 50 J. Zhao, F. Liu, Z. Wang, X. Cao and B. Xing, Heteroaggregation of graphene oxide with minerals in aqueous phase, *Environ. Sci. Technol.*, 2015, **49**, 2849.